J Mol Model (2005) 12: 34–41
DOI 10.1007/s00894-005-0001-2

ORIGINAL PAPER

Elena Ermakova

Lysozyme dimerization: brownian dynamics simulation

Received: 24 August 2004 / Accepted: 12 May 2005 / Published online: 18 August 2005

Abstract The lysozyme dimerization reaction has been studied within the framework of encounter-complex (EC) formation theory using the MacroDox software package. Two types of energetically favorite ECs were determined. In the first of them, active-center amino acids of lysozyme take part in the complex formation or the second molecule blocks accessibility to active center sterically. Epitope amino-acid residues are involved in the complex of type II. The existence of both types of complexes does not contradict experimental data. Dimer-formation rate constants for different kinds of EC were calculated. Increasing the pH from 2.0 to 10.0 decreases the total positive lysozyme charge and eliminates the unfavorable repulsive electrostatic interaction. The rate constant of EC formation is inversely proportional to the protein total charge. The association rate constant was also enhanced by an increase of ionic strength that screened repulsive electrostatic interaction between positively charged proteins.

Keywords Brownian dynamics simulation · Lysozyme · Dimerization · Electrostatic interactions

Introduction

Understanding the nature of recognition of two protein molecules and the mechanism of protein–protein interaction is a key to understanding such processes as antibody–antigen recognition, signal transduction and inhibition of enzymes by intercellular inhibitor proteins.

The increasing number of publications studying protein interactions using computer simulations underlines the actuality of the problem, as well as the applicability of these methods for such studies [1–5].

It has been shown convincingly [6–8] that electrostatic effects are determinants in protein–protein association. However, in most cases studied, the molecules were oppositely charged [1, 8]. Lysozyme has an isoelectric point of pH 11. However, lysozyme is known to self-associate at pH higher than 4 [9]. Under these conditions, it has a net positive charge that should prevent association. Therefore, the effect of electrostatic interactions on lysozyme association must be clarified.

The association of lysozyme has been studied experimentally using light and neutron scattering [10–12], NMR diffusion measurements [13, 14], magnetic relaxation dispersion [15], and theoretically by Monte Carlo [16] and molecular dynamics simulations [17]. The Brownian Dynamics (BD) method has been used to study the interaction of lysozyme with a positively charged surface [18]. It has been shown that positively charged hen egg white lysozyme can be adsorbed onto the positively charged surface. BD has also been used to calculate the association rate constant for lysozyme/antigen association [19].

It is well known that the complex-formation process has two stages. The first is when the two molecules diffuse into each other and an intermediate encounter complex (EC) is created and the second is when the system is transformed from EC to the binding complex. An EC is defined [5] in terms of an ensemble of configurations of the two proteins. This ensemble of configurations has two properties; it dissociates much more slowly than it evolves to the bound complex, and it is accessible by diffusion.

The goal of this work is to study the first stage of lysozyme dimerization using the BD simulation method.

Brownian Dynamics is widely used for studying the kinetics and energetics of rigid-body protein–protein association [19–21]. This method works properly when the complex structure is known, and a reaction criterion (RC) is established based on the known structure [5, 21]. Ouporov et al. [20] have used the BD method to study

E. Ermakova
Kazan Institute of Biochemistry and Biophysics RAS,
420111 Kazan, P.O. Box 30,
Russia
E-mail: ermakova@mail.knc.ru
Tel.: +7-8432-319037
Fax: +7-8432-927347

protein–protein interaction without biasing the RC for particular types of complexes. The aim of our work is twofold; firstly to define the most energetically favorable lysozyme dimer structures without previously defining the RC and, secondly, to estimate the probability of formation of such complexes using the RCs.

Material and methods

Lysozyme dimerization was studied using the program package MacroDox version 3.0.0 [22]. This package was used to assign the titratable charges for the protein, solve the linearized Poisson–Boltzmann equation, and run the BD simulations. The details of the algorithms are given in Northrup et al. [23, 24]. The shortcomings of BD simulation methods generally and of the MacroDox program particularly, have been discussed widely in the literature [21, 25]. The main disadvantage of the method is the calculation for fixed protein structures. In order to compensate this shortcoming partially, we carried out all calculations for three initial lysozyme structures. The atomic coordinates of hen egg-white lysozyme (HEWL) (entry codes are 1lys, 5lyz, 1lza) were obtained from the Protein Data Bank at Brookhaven National Laboratory [26].

Using these atomic coordinates, charges of titratable amino acids were assigned for solvent ionic strength of 0.1 M, temperature of 298 K, and pH values ranging from 2.0 to 10.0 by the Tanford–Kirkwood method [27, 28]. Electrostatic interactions (long-range forces) between two reactants were included in our model as a basic feature along with short-range repulsive forces. No hydrophobic forces were modeled and flexibility of the proteins was not allowed during the simulations. The electrostatic potential around the lysozyme molecules was determined by solving the linearized Poisson–Boltzmann (PB) equation numerically using the Warwicker and Watson [29] method, implemented in the program MacroDox. The PB equation was solved for two cubic lattices, and the center of mass (COM) of one lysozyme molecule was placed at the origin of the lattice. The resolution was equal to 0.9 Å for the inner grid and to 2.7 Å for the outer one. The dielectric constant used in the calculations was set to 4 for proteins and 78 for solvent.

Trajectories were calculated using the Ermak–McCammon algorithm [30]. At the beginning of each trajectory, the COM of the second protein was placed randomly on a spherical surface with radius b (70 Å in this study) from the COM of the first protein. Then, the second molecule was allowed to rotate and translate. If the distance between COMs of two molecules reached the escape radius c (200 Å), the trajectory was terminated.

The coordinates of the second particle at time of $t+\tau$ were defined according to equation:

$$r(t+\tau) = r(t) + \frac{D\tau}{kT}F + R(\tau)$$

Here D is the spatially isotropic translational diffusion coefficient for relative motion, F is the direct interparticle (electrostatic) force and R (τ) is the random displacement vector used to simulate solvent-mediated Brownian translational motion. A similar equation was used to describe the rotational motion of the particles. In our calculations, D was equal to 0.026 $Å^2\ ps^{-1}$ and the rotational diffusion coefficient was $0.33\times10^{-4}\ ps^{-1}$.

An encounter complex is formed when two atoms from different proteins come as close as X Å, where X is the "reaction criterion." In this case, the trajectory is considered to be successful. The number of successful trajectories is used to estimate the rate constant for association. The rate constant for lysozyme dimerization was calculated according to Northrup's equation [31, 32], derived using Smoluchovski theory [33]:

$$k = k_D(b)\frac{p}{1-(1-p)k_D(b)/k_D(c)}$$

$$k_D(x) = 4\pi x D N_A$$

Here p represents the number of successful trajectories as a fraction of trajectories collected, and N_A is Avogadro's number.

Results and discussion

The distribution of electrostatic potential (EP) around lysozyme is primarily determined by charged amino-acid residues located on its surface. While the net charge of the lysozyme molecule is positive, there are regions of strong positive potential, and also small patches of negative potential, at the lysozyme surface. One of these patches is formed by the Glu35 and Asp52 residues and is located in the pocket of the protein. Others are formed by the single amino acids: Asp18, Asp48, Asp66, Asp101, and Asp119. The alternating pattern of positive (blue) and negative (red) electrostatic potential at the surface of lysozyme is shown in Fig. 1.

Calculations were carried out for three initial structures (1lys, 5lyz, and 1lza). Two kinds of simulations were performed. In the first of them, 250,000 trajectories were run for each structure and complexes with negative interaction energy were analyzed without biasing the RC for particular types of complexes. The second kind of simulation was run for 25 different predefined ECs and the rate constants for formation of each complex were calculated. Solvent-accessible surfaces were calculated for all lysozyme amino-acid residues using the MOLMOL program [34] (data not shown). Contact pairs were chosen from the charged amino-acid residues most exposed in solution.

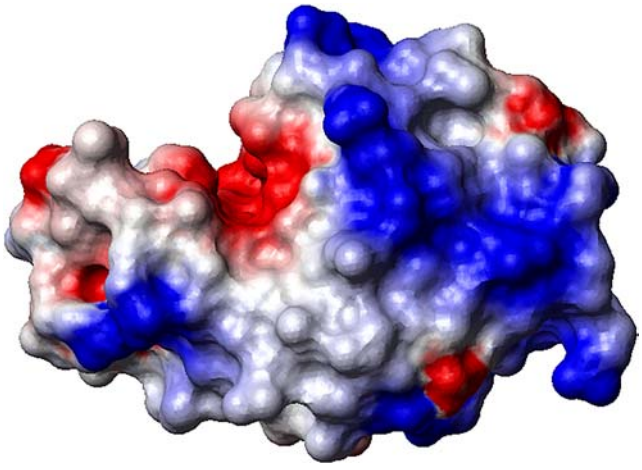

Fig. 1 The distribution of electrostatic potential at the lysozyme surface. The surface, rendered using MOLMOL [34] maps the electrostatic potential on scale from -0.5 kcal mol^{-1} (*red*) to 0.5 kcal mol^{-1} (*blue*)

Fig. 2 The distribution of the second HEWL molecule COM around the first molecule of HEWL. Each red dot represents the second lysozyme molecule COM in encounter complexes. The first molecule is shown as a secondary structure schema. Picture was created using MOLMOL [34] program

In spite of the much different experimental work [35–41] devoted to lysozyme investigations, a direct comparison of our results with experiment is difficult because of the different experiment conditions. All further comparisons in this article have qualitative character.

Energetically favorable complexes

For the first kind of simulation, structures with negative electrostatic interaction energies were saved for subsequent analysis. Analysis of the most energetically favorable complexes (electrostatic energy less than -4 kcal mol^{-1}) shows that the dominant binding region of one lyzosyme molecule to another is determined by the attraction of negatively charged patches of one lysozyme molecule to the positively charged regions of the second lysozyme molecule.

This conclusion is based on the determination of the occurrence frequency of each amino acid involved in the intermolecular contact. The residues of the lysozyme molecule Lys33, Glu35, Asp48, Asp52, Arg61, Arg73, Asp101, Arg112, Arg116, and Arg128 are frequently involved in complex formation, and pairs of residues Lys33–Asp101, Glu35–Arg61, Glu35–Arg73, Asp52–Arg61, Asp52–Arg73, Arg112–Asp48, Lys116–Asp48, Asp48–Arg73, and Asp48–Arg128 are formed most frequently.

The summary distribution of the first lysozyme molecule COM around the second lysozyme molecule for all three structures is shown in Fig. 2. The central molecule is represented as the secondary structure scheme, for the second molecules only the COM are shown. Analysis of the most energetically favorable complexes shows that we can recognize two main groups of complexes, type I and type II.

In the first of them (type I) active-center amino acids of lysozyme take part in complex formation or the accessibility to the active center is blocked sterically by the second molecule. Complexes of type II are characterized by their free active centers.

Complexes of type I are formed by interactions between the positively charged nitrogens of Lys33, Arg112, and Arg114 and negatively charged oxygens of Glu35 and Asp52 of the first molecule and negatively charged oxygens of Asp101 and Asp48 and positively charged nitrogens of Arg61 and Arg73 of the second lysozyme molecule. Additional stabilization of these complexes is achieved by a second salt bridge between second or third pairs with distances around 3–6 Å . The most intimate salt bridges for such complexes are established between Arg73–Glu35, Asp52–Arg61, Asp52–Arg73, Arg112–Asp48, and Asp101–Arg114. The formation of contacts Lys33–Asp48,Arg112–Glu35,Glu35–Arg73, and Arg73–Asp101 provides the main contribution to the energetic stability of type I complexes. A typical complex of type I with an electrostatic interaction energy of -4.75 kcal mol^{-1} is shown in Fig. 3. The contact area for this complex is 224 Å^2 .

The formation of type I complex was fixed for all three initial structures.

An analysis of macromolecular structures (http://pqs.ebi.ac.uk) that can be formally described as lysozyme dimers (solvent accessible surface area (ASA) decreases significantly upon complex formation, negative interaction energy) allows them to be divided into three groups. The first one (group I) has symmetry group C2 or P6122, and the dimerization locks the lysozyme active center. This group includes 2ihl (Arg73 creates a hydrogen bond with Ile98, Arg73 and Asp48 have close contacts with Asp101 and Arg112, respectively), 2lz2, and 3lz2 (Asn74–Gly102 and Trp62–Trp62 hydrogen

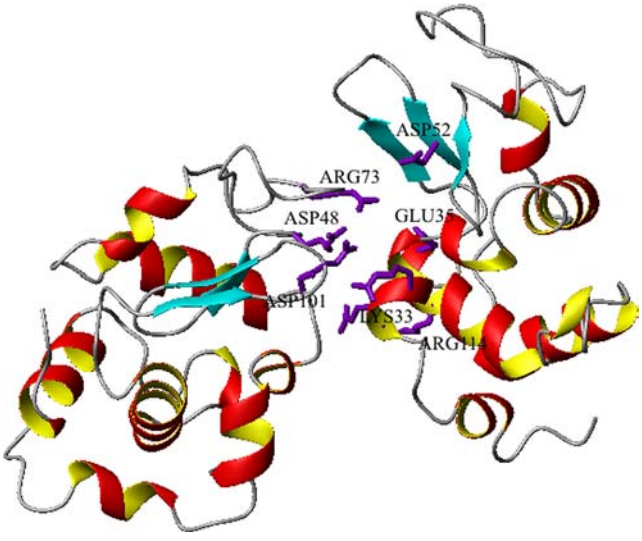

Fig. 3 The structure of type I EC. A ribbon representation of two HEWL molecules, contact amino-acid residues (Lys33, Glu35, Asp52, and Arg114 of the first HEWL molecule and Arg73, Asp48, and Asp101 of the second HEWL molecule) are shown explicitly

bonds are formed) structures and can be compared with the calculated dimers of type I. The second group (group II) of dimers has P6122 symmetry, where the active center is not locked but the access to it is sterically hampered. In this case, hydrogen bonds are formed between Glu121–Glu121, Asn19–Asn27, and Asp119–Lys13. Representatives are the structures 1hhl and ldkj. The most numerous group of dimers (group III) (space group is P3121 or P43212) is the one with a free active center. On formation of these dimers (e.g., 193l, 5lyz, 4lyz, 1lmq, and 2lyz) the hydrogen bonds between Asp66–Asn39, Arg68–Asn44, Arg68–Thr43, and Arg45–Asn44 are formed.

We believe that the calculated EC of type I can be transformed into the binding complex of the first group as a result of subtle turning and specific orientation of two proteins and creating additional hydrogen bonds and ion bridges.

Formation of the first type complex agrees with the observed decrease in activity of the enzyme dimer compared to the monomer. This fact was revealed by Sorrentino et al. [37]. Hashimoto et al. [39] have shown by light-scattering-intensity measurements that the enzymatic activity of the dimer is reduced to about 30% of that of the intact enzyme. NMR experiments [38] revealed the participation of tryptophan 62 in the self-association of HEWL, which also coincides with the formation of type I complexes. Norton and Allerhand's [38] results indicate that self-association of lysozyme is not accompanied by any general conformational change, and that binding of a lanthanide ion (at the metal-ion binding site near the carboxylate groups of Asp52 and Glu35) strongly suppressed self-association.

Formal analysis of type II structures is complicated by the presence of many different dimer conformations and by the dependence of these conformations on the initial macromolecular structure. The variety of different energetically profitable dimer conformations coincides with the fact that lysozyme can form dimers as well as more complicated oligomers (up to 16 monomers in one oligomer) [36].

On formation of complexes of type II, the main role belongs to epitope amino-acid residues. ECs with participation of the epitope amino-acid residues (Arg128, Leu129, Arg125, Lys13, Asp119) were also observed for all three initial molecular structures. Depending on the second protein orientation, "head-to-tail" or "head-to-head" complexes can be formed.

For complexes of type II, the most intimate salt bridges are formed by positively charged nitrogens from Arg128 residues of the first lysozyme molecule and negatively charged oxygens from Asp48, Asp101, or Asp119. Formation of contacts Arg128-Asp48, Arg128-Asp101 provides the main contribution to the complex stability. A typical complex of type II with electrostatic interaction -6.3 kcal mol^{-1} is shown in Fig. 4. The contact area for this complex is very small (85 Å^2) and involves just Arg128 and Leu129 residues of one molecule and Asp48 and Arg61 residues of the second.

"Head-to-tail" or "head-to-head" dimers were not found among known dimer structures, but their formation has been observed experimentally. A "head-to-tail" contact between the associating sites was inferred from dialysis studies of lysozyme self-association [40]. Yonezawa et al. [12] studied the amyloid fibril formation of HEWL and showed that the distance between lysozyme monomer centers in the lysozyme dimer is close to

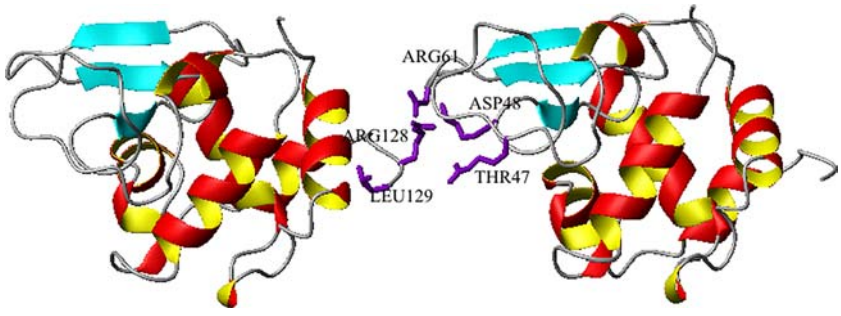

Fig. 4 The structure of type II EC. A ribbon representation of two HEWL molecules, contact amino-acid residues (Arg128 and Leu129 of the first HEWL molecule and Arg61, Thr47, and Asp48 of second HEWL molecule) are shown explicitly

the largest dimension of HEWL. They suggested that the association occurs at one end of the long axis of the molecule and the resulting dimer has an elongated shape that is not in conflict with our calculations.

However, for all initial structures there are some additional stable complexes. Their formation depends on the initial structure. For example, counting on the 1lza structure has revealed the formation of a complex similar to the 1dkj structure and Arg125–Asp119, Asp119–Arg125 contact pairs have been created. However, this complex has not been defined for other structures.

The formation of complexes that can be transformed into binding complex of group III has not been settled in our calculations.

Steric accessibility and influence of the side-chain conformation

The influence of side-chain conformation and of their motion on the EC formation and especially on the transformation process from EC to binding complex has still not been clarified.

Gabdoulline and Wade [21] mentioned briefly that the BD simulation for rigid protein structure depended in great part on the specific initial molecular structure for which the calculation was performed. The calculation results for different structures can be different by the order of magnitude.

Nielsen et al. [42] have used the WHAT IF program for pK calculation for the lysozyme active center amino acids for 41 lysozyme initial structures and have shown that the calculated pK depended on the initial structure of the macromolecule. The pK for Glu35 ranges between 4.29 and 7.82, and for Asp52 between 1.72 and 6.57.

In the theory of BD simulations it is assumed [2, 5] that movement of side chains is faster than protein diffusion, that is why the counting of EC for different rigid structures and average meanings of reaction constants should give a more realistic picture of EC formation and the rates of the different types of complex formation.

We assume that the numerical results of rate-constant calculations would depend on the calculation parameters and, in particular, on the definition of the EC and the RC. However, we believe that the qualitative picture reveals the influence of electrostatic interactions on the preferred lisozyme dimer structures. In order to analyze the formation probabilities of different complexes of lysozyme, the second kind of calculations was carried out and lysozyme dimerization-reaction rate constants were calculated.

The formation probabilities of 25 different complexes were estimated. The distance between specific atoms was determined as RC. 50,000 trajectories for each type of RC were run. The results are listed in Table 1. Contact atoms of the first and the second lysozyme molecules and the EC formation probability for three initial structures are shown (the RC is 5 Å). The two last columns of Table 1 show the average meaning of the

Table 1 EC formation probabilities and the average rate constants for different kinds of contact groups and 3 lysozyme structures

	First protein contact group	Second protein contact group	Probability (%)			Avg. probability (%)	Avg. rate constant $\times 10^7$ (M^{-1} s^{-1})
			1lys	5lyz	1lza		
1	OD2 Asp119	NH2 Arg73	0.24	0.54	0.54	0.44	9.2
2	NH2 Arg73	NH2 Arg128	0.50	0.52	0.21	0.41	8.6
3	NH2 Arg73	OD1 Asp87	0.39	0.57	0.19	0.38	7.9
4	NH2 Arg73	OD2 Asp48	0.84	0.13	0.14	0.37	7.7
5	OD2 Asp119	NH1 Arg45	0.07	0.30	0.66	0.34	7.1
6	NH1 Arg45	NH2 Arg73	0.29	0.30	0.23	0.27	5.6
7	OD2 Asp119	NH2 Arg114	0.10	0.17	0.36	0.21	4.4
8	OD2 Asp119	NH1 Arg14	0.09	0.31	0.21	0.20	4.2
9	NH2 Arg128	O Pro70	0.23	0.27	0.07	0.19	4.0
10	NH2 Arg73	NH1 Arg68	0.34	0.11	0.10	0.19	4.0
11	NH2 Arg128	OD2 Asp48	0.29	0.08	0.09	0.15	3.2
12	O Pro70	NH1 Arg68	0.28	0.05	0.09	0.14	2.9
13	NH1 Arg14	OD1 Asp87	0.07	0.19	0.09	0.12	2.4
14	NH1 Arg45	OD1 Asn44	0.10	0.14	0.10	0.11	2.3
15	OD2 Asp119	NZ Lys13	0.03	0.09	0.15	0.09	1.9
16	NH1 Arg125	O Pro70	0.07	0.10	0.08	0.09	1.9
17	OD1 Asp101	NH2 Arg114	0.23	0.006	0.02	0.08	1.7
18	NZ Lys97	OD1 Asp87	0.008	0.11	0.04	0.05	1.0
19	NH2 Arg112	NH1 Arg61	0.04	0.07	0.04	0.05	1.0
20	NH2 Arg125	OD2 Asp48	0.07	0.01	0.05	0.04	0.8
21	OD2 Asp18	NH2 Arg21	0.08	0.02	0.02	0.04	0.8
22	NZ Lys33	OD1 Asp101	0.08	0.002	0	0.03	0.6
23	OE1 Glu35	NH2 Arg73	0.05	0.02	0.002	0.02	0.5
24	OD2 Asp52	NH2 Arg73	0.04	0.03	0.004	0.02	0.5
25	NZ Lys97	OD1 Asp101	0.02	0.004	0	0.01	0.2

probability and the average rate constant of EC formation. Calculations were carried out at pH 7.0 and a solution ionic strength of 0.1 M.

Table 1 shows a complicated dependence of the EC formation probability on the protein electrostatic potential and on the steric accessibility of amino-acid residues. The rates calculated with different fixed structures vary widely. However, fast motion of side-chain amino acids in solution must average their spacial arrangement and smooth this difference. The high activity of Arg73, Arg128, Asp48, and Asp119 and low activity of Glu35, Asp52, and Asp66 in formation of contact pairs are common for all initial structures studied.

A comparative analysis of the data of Table 1 and complexes of type I and of type II reveals that complexes with formation of pairs of residues Asp48–Arg73 and Asp48–Arg128 have high formation probabilities and are energetically stable. At the same time, the probability that two positively charged amino acids such as Arg73 and Arg128 have a close contact is high enough, but the interaction energy of such complexes is positive and this EC is unstable (the average energy of 251 complexes, where the distance between NH2 Arg73 and NH2 Arg128 atoms was less then 5 Å, equals 1.4 kcal mol^{-1}). The residues Glu35 and Asp52 which generate negative EP and demonstrate binding activity to another lysozyme molecule, are not exposed to solution and are not fully accessible from solution. All ECs listed in Table 1 are accessible by translational and rotational diffusion of proteins with different probabilities but the probability of transformation of these complexes into the bound complex is determined by the interaction energy of the two proteins and short-range forces. The rate constants obtained can be considered as the upper limit of lysozyme dimerization rate constants.

Ionic strength and pH dependence of the association rate

Changing the solution pH from acid to basic causes deprotonation of His, Glu, and Asp residues and decreases the total positive lysozyme charge and alters the electrostatic potential pattern on the protein surface. The net charge on a protein at any given pH is determined by the p*K* values (p*K*s) of the ionizable groups [27, 28]. The surface-accessibility-modified Tanford–Kirkwood (TK) method encoded in MacroDox was used to determine the protonation status of each titratable residue in the protein at different pH and ionic strengths. This method produces results similar to other theoretical methods and is widely used for p*K* calculations [3, 4, 20]. Typically, theoretical methods give results that are within ± 1 pH unit of the experimental pI [43, 44]. The lysozyme pI in our calculations is 10.2 ± 0.1, (for comparison, a multiconformation continuum electrostatics method calculation gives 10.5 [45]); the experimental value is 11.2 [39].

Figure 5 shows the lysozyme total charge dependence and dimerization rate constant on solution pH (pH varied in a diapason from 2.0 to 10.0). Calculations were performed for the 1lza initial structure and the oxygen atom of Asp48 and nitrogen atom of Arg73 were taken as a contact group. The character of the dependence EC formation rate constant on solution pH is identical for all initial structures.

One can see that while the pH increases the association reaction is enhanced. Increasing the pH decreases the total positive lysozyme charge and eliminates the unfavorable repulsive electrostatic interaction and the rate constant of EC formation is inversely proportional to the protein total charge.

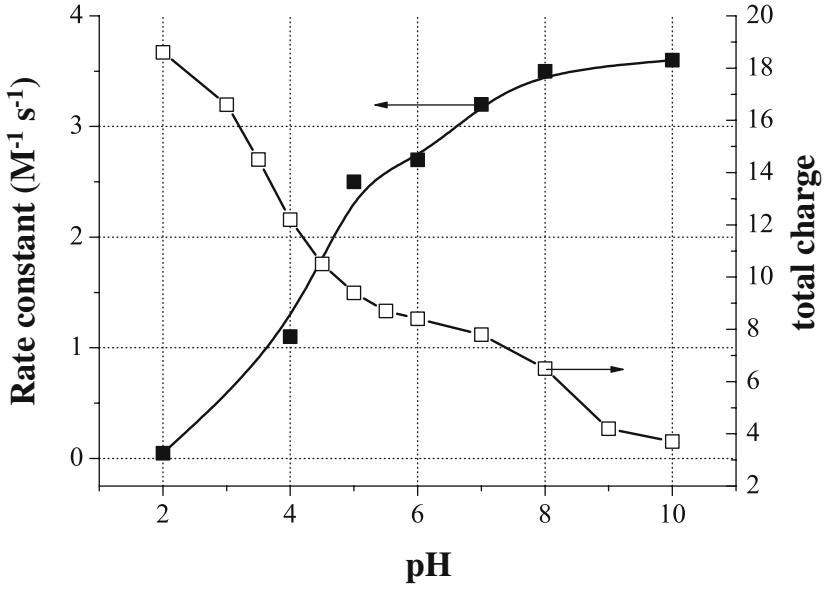

Fig. 5 HEWL total charge (*open squares*) and lysozime dimerization rate constant (*solid circles*) dependence on solution pH (ionic strength equals 0.1 M). Rates are given in units of 10^7 M^{-1} s^{-1}

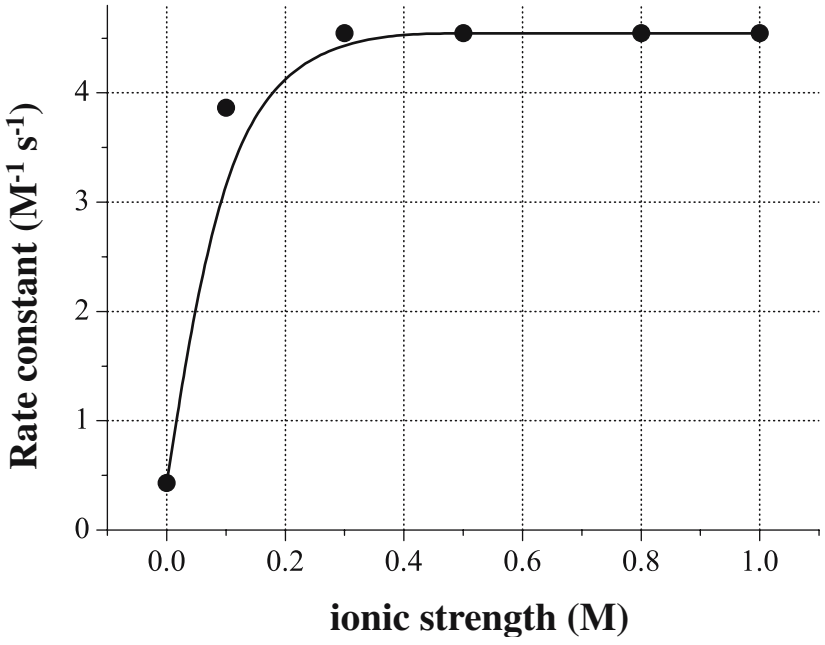

Fig. 6 Ionic strength dependence of lysozime association rate constant (pH equals 7.0). Rates are given in units of 10^7 M^{-1} s^{-1}

Increasing the ionic strength that screens repulsive electrostatic interactions between positively charged proteins also enhances the association rate constant. The dependence of the rate constant of EC formation on solution ionic strength is shown in Fig. 6 (the oxygen atom of Asp48 and nitrogen atom of Arg73 were taken as a contact group, the pH was equal to 7.0). The character of the dependence of the EC formation rate constant on solution ionic strength is identical for all initial structures. Dialysis kinetics measurements have also indicated that dimerization increases with the ionic strength of the solution [36]. The effect of salt concentration on amiloid fibril formation of HEWL has recently been investigated experimentally [35]. Fujiwara et al. [35] revealed that the time required for HEWL gelation decreases with increasing NaCl concentration. This result agrees with our calculations.

Conclusion

Analysis of proteins electrostatic interaction energies allows us to define the most energetically favorable structures of encounter complexes. Monomer orientation in such complexes is determined by the protein surface-charge distribution. The dominant binding region of one lyzosyme molecule to another was determined by the attraction of negatively charged patches of the first lysozyme molecule to the positively charged regions of the second. However, EC formation probability also depends on the steric accessibility of the amino acids participating in the complex formation by translational and rotational diffusion of the interacting proteins. The rate constant dependence on pH and ionic strength of solution confirms the electrostatic nature of lysozyme dimerization.

Acknowledgements The author is very grateful to Dr. S. Northrup for providing her with the MacroDox package programs and Dr. I. Nesmelova (Minnesota University) for critical reading of this manuscript. This work was supported by the Russian Foundation for Basic Research grant 03-04-96276p2003tatarstan and NIOKR AN RT grant 03.3-10.227.

References

1. Gabdoulline RR, Wade RC (2001) J Mol Biol 306:1139–1155
2. Gabdoulline RR, Wade RC (2002) Curr Opin Struct Biol 12:204–213
3. Elcock AH, McCammon JA (2001) Biophys J 80:613–625
4. Pearson DC, Gross EL (1998) Biophys J 75:2698–2711
5. Gabdoulline RR, Wade RC (1999) J Mol Recognit 12:226–234
6. Sinha N, Smith-Gill SJ (2002) Curr Protein Pept Sci 3:601–614
7. Elcock AH, Sept D, McCammon JA (2001) J Phys Chem B 105:1504–1518
8. Camacho CJ, Weng Z, Vajda S, DeLisi C (1999) Biophys J 76:1166–1178
9. Sophianopoulos AJ, van Holde KE (1964) J Biol Chem 239:2516–2524
10. Kuehner DE, Heyer C, Ramsh C, Fornefeld UM, Blanch HW, Prausnitz JM (1997) Biophys J 73:3211–3224
11. Mischol M, Rosenberger FJ (1995) J Chem Phys 103:10424–10432
12. Yonezawa Y, Tanaka Sh, Kubota T, Wakabayashi K, Yutani K, Fujiwara S (2002) J Mol Biol 323:237–251
13. Nesmelova IV, Fedotov VD (1998) Biochim Biophys Acta 1383:311–316
14. Price WS, Tsuchiya F, Agata Y (2001) Biophys J 80:1585–1590
15. Gottshalk M, Halle B (2003) J Phys Chem B 107:7914–7922
16. Carlsson F, Malmsten M, Linse P (2001) J Phys Chem B 105:12189–12195
17. Stocker U, Spiegel K, van Gunsteren WF (2000) J Biomol NMR 18:1–12

18. Ravichandran S, Madura JD, Talbot J (2001) J Phys Chem B 105:3610–3613
19. Altobelli G, Subramaniam Sh (2000) Biophys J 79:2954–2965
20. Ouporov IV, Knull HR, Thomasson KA (1999) Biophys J 76:17–27
21. Gabdoulline RR, Wade RC (1997) Biophys J 72:1917–1929
22. Northrup SH, Laughen T, Stevenson G (1997) MacroDox macromolecular simulation program. Tennessee Technological University, Cookeville, TN
23. Northrup SH, Boles J, Reynolds J (1988) Science 241:67–70
24. Northrup SH, Boles JO, Reynolds JCL (1987) J Phys Chem 91:5991–5998
25. Gross EL (2004) Biophys J 87:2043–2059
26. Bernstein FC, Koetzle TF, Williams GJB, Meyer EF, Brice MD, Rogers JR, Kennard O, Shimanouchi T, Tatsumi M (1977) J Mol Biol 112:535–542
27. Tanford C, Kirkwood JG (1957) J Am Chem Soc 79:5333–5539
28. Matthew JB, Gurd FRN (1986) Methods Enzymol 130:413–436
29. Warwicker J, Watson HC (1982) J Mol Biol 157:671–679
30. Ermak DL, McCammon JA (1978) J Chem Phys 69:1353–1360
31. Northrup SH, Allison SA, McCommon AA (1983) J Chem Phys 80:1517–1524
32. Zhou H-X (1990) J Phys Chem 92:3092–3095
33. Smoluchowski MV (1916) Phys Z 17:557–571
34. Koradi R, Billeter M, Wuthrich K (1996) J Mol Graphics 14:51–55
35. Fujiwara S, Matsumoto F, Yonezawa Y (2003) J Mol Biol 331:21–28
36. Wilson LJ, Adcock-Downey L, Pusey ML (1996) Biophys J 71:2123–2129
37. Sorrentino S, Yakovlev GI, Libonati M (1982) Eur J Biochem 124:183–189
38. Norton RS, Allerhand A (1977) J Biol Chem 252:1795–1798
39. Hashimoto S, Seki H, Masuda T, Imamura M, Kondo M (1981) Int J Radiat Biol Relat Stud Phys Chem Med 40:31–46
40. Hampe OG, Tondo CV, Hasson-Voloch A (1982) Biophys J 40:77–82
41. Frare E, Polverino de Laureto P, Zurdo J, Dobson CM, Fontana A (2004) J Mol Biol 340:1153–1165
42. Nielsen JE, McCammon JA (2003) Protein Sci 12:313–326
43. Shaw KL, Grimsley GR, Yakovlev GI, Makarov AA, Pace CN (2001) Protein Sci 10:1206–1215
44. Patrickios CS, Yamasaki EN (1995) Anal Biochem 231:82–91
45. Georgescu RE, Alexov EG, Gunner MR (2002) Biophys J 83:1731–1748